European Journal of Pharmaceutical Sciences 37 (2009) 98–105

Contents lists available at ScienceDirect

European Journal of Pharmaceutical Sciences

journal homepage: www.elsevier.com/locate/ejps

PEG conjugated N-octyl-O-sulfate chitosan micelles for delivery of paclitaxel: In vitro characterization and in vivo evaluation

Guowei Qu [1], Zhong Yao [1], Can Zhang*, Xiaoli Wu, Qineng Ping*

College of Pharmacy, China Pharmaceutical University, Nanjing 210009, PR China

ARTICLE INFO

Article history:
Received 11 August 2008
Received in revised form 4 November 2008
Accepted 13 January 2009
Available online 22 January 2009

Keywords:
PEGylated chitosan
Micelles
Paclitaxel
Pharmacokinetics
Tissue distribution

ABSTRACT

A series of novel chitosan derivatives (mPEGOSC) with hydrophobic moieties of octyl and hydrophilic moieties of sulfate and polyethylene glycol monomethyl ether (mPEG) groups were synthesized. The values of critical micelle concentration (CMC) were found to be 0.011–0.079 mg/ml, and the log CMC was linearly relative to four structure parameters, degree of substitution (DS) of chitosan unit, sulfate group, PEG unit and octyl group by mole per kilogram. Paclitaxel (PTX)-loaded micelles were prepared with the highest loading rate of 42.6%. In vivo–in vitro correlations of PTX-loaded micelles was designed and conducted, including interaction of the drug-loaded micelles with protein and the kinetics of PTX-loaded micelles below CMC. mPEG2000 and mPEG5000 on the surface of micelles provided stronger inhibition to protein adsorption compared with mPEG1100, and the micelles based on mPEGOSC with higher DS of chitosan unit (mol/kg) shown slower dissociation when diluted below CMC. The pharmacokinetic research of PTX-loaded micelles based on OSC (PTX-OSC), PTX-loaded micelles based on mPEGOSC (PTX-mPEGOSC) and Taxol® was carried out in rat. The area under the plasma concentration time curve (AUC $(0–t_n)$) of PTX-mPEGOSC2000M was 10.21 ± 2.12 μg h/ml, which were 2.93 times higher than PTX-OSC and 0.83 times lower than Taxol®. Rate constant of distribution phase (α) and rate constant of elimination phase (β) were analyzed by linear regression with the absorbance of protein to micelles (A) and the fraction of intact micelles at 10 min ($f_{t,\,10\,\mathrm{min}}$). The tissue distribution studies in mice indicated that PTX-mPEGOSC2000M micelles were phagocytized less than PTX-OSC micelles by reticuloendothelial system (RES). Furthermore, higher targeting efficiency of PTX-mPEGOSC2000M to uterus (including ovary) was estimated. On the basis of these results, it could be a promising PTX-encapsuled formulation for the chemotherapy of ovarian cancer.

1. Introduction

Paclitaxel (PTX), the first of a new class of microtubule stabilizing agents, is one of the most successful anticancer drugs and shows potency against a broad spectrum of cancers, especially carcinomas of the breast and ovary and lung (Panchagnula, 1998; Singla et al., 2002). However, the strong hydrophobicity of paclitaxel drastically limited its use in natural form. The commercial dosage form of paclitaxel for administration, Taxol®, contains 50% Cremophor® EL to increase its solubility. Unfortunately, Cremophor® EL, which is used as solubilizing agent, was shown to be biologically active and induces severe side effects like dyspnea, flushing, rash and urticaria up to 30% of the treated patients (Wang et al., 2005). In addition, significant toxicities, especially to the rapidly proliferating cells, manifested as myelosuppression, peripheral neuropathy, etc., limited the application of paclitaxel in cancer therapy, which was substantially ascribed to the non-specific distribution among the tissues indiscriminately (Marupudi et al., 2007). Hence, many attempts have been made to find alternative carriers to deliver paclitaxel to the focus tissue as much as possible without inducing adverse reactions in the healthy tissues.

Numerous drug delivery systems based on parenteral emulsions (Kan et al., 1999), liposomes (Ceruti et al., 2000), water-soluble prodrugs (Wrasidlo et al., 2002), nanoparticles (Hawkins et al., 2008) and polymeric micelles (Hennenfent and Govindan, 2005; Croy and Kwon, 2006; Mahmud et al., 2007) were extensively studied and evaluated in the field of cancer therapy, particularly, and the polymeric micelles have received much attention. Further, three polymeric micelle formulations of PTX were in clinical trials. PAXCEED® (Zhang et al., 1996), the first polymeric micelle formulation of PTX, was prepared using PEO-*b*-PDLLA. Compared with Taxol®, 5.5-fold decrease in the AUC of PTX in blood after

* Corresponding authors. Tel.: +86 25 85333041; fax: +86 25 85333041.
E-mail address: zhangcancpu@yahoo.com.cn (C. Zhang).
[1] These authors contributed equally to this work.

0928-0987/$ – see front matter © 2009 Elsevier B.V. All rights reserved.
doi:10.1016/j.ejps.2009.01.004

intravenous administration was found and attributed to the rapid loss of PTX from the micellar carrier (Zhang et al., 1997). Genexol®-PM (Kim et al., 2001), which was also prepared using PEO-*b*-PDLLA, a 1.35-fold lower AUC in plasma was obtained despite a 2.5-fold increase in the administered dose. Meanwhile, the CL (total plasma clearance) and Vd (apparent distribution volume) values in steady state increased more than 3-fold. So far, NK-105, which was constructed with PEO-*b*-poly(4-phenyl-1-butanoate) L-aspartamide (PEO-*b*-PPBA), was the only polymeric micelle formulation of PTX which successfully achieved passive targeting properties. In comparison with Taxol®, NK-105 showed an 86-fold increase in AUC in plasma, an 86-fold decrease in CL and a 15-fold decrease in Vdss (steady state) (Hamaguchi et al., 2005). In our earlier papers (Zhang et al., 2008a,b), amphipathic chitosan derivate, N-octyl-O-sulfate chitosan (OSC) was synthesized and estimated in animal models as a paclitaxel carrier for intravenous administration. Although the PTX-loaded micelle based on OSC (PTX-OSC) kept similar antitumor efficacy as Taxol® and significantly reduced the toxicity PTX, the area under the plasma concentration time curve (AUC) of PTX-OSC was 3.6-fold lower than that of Taxol® and most of the PTX were distributed in the tissues rich in RES, as liver, spleen and lung. In this study, polyethylene glycol monomethyl ether (mPEG) group was introduced into the 2-NH_2 of OSC due to its superior biocompatibility and hydrophilicity (Otsuka et al., 2003), the drug-loaded micelles assembled spontaneously based on the new materials were anticipated to prolong circulation time, minimize non-specific uptake, allow for specific tumor-targeting through the enhanced permeability and retention effect by passive targeting (Vlerken et al., 2007). The pharmacokinetic parameters (β, rate constant of elimination phase) of PTX-mPEGOSCs were estimated with the assistant of in vitro stability experiment, dissociation kinetics of micelles below CMC. In the dissociation study of micelles below CMC, two dynamics parameters, the dissociation rate constant in the initial 30 s (k) and the fraction of intact micelles at 10 min ($f_{t,\,10\,\mathrm{min}}$), were investigated as a function of degree of substitution (DS) of chitosan unit (mol/kg) of corresponding chitosan derivates. Moreover, linear regressions between logarithmic β and $f_{t,\,10\,\mathrm{min}}$ were performed, high linearity were observed. Furthermore, the pharmacokinetics, tissue distribution of the PTX formulations Taxol®, PTX-OSC, PTX-mPEGOSC was compared.

2. Materials and methods

2.1. Materials

Chitosan was provided by the Nantong Suanglin Biochemical Ltd., China, with deacetylation degrees of 50% and viscosity average molecular weight of 65,000 D. Pyrene (>99%) and polyethylene glycol monomethyl ether (mPEG) with the molecular weight of 1100, 2000 and 5000 were purchased from Sigma (Milwaukee, WI, USA). The other reagents were analytical grade and used without further purification. Double distilled water was used in this study. N-octyl-O-sulfate chitosan (OSC) was synthesized by our group and the chemical constitution was shown in Fig. 1 (Zhang et al., 2003, 2004).

2.2. Animals

Sprague–Dawley (SD) rats were obtained from the Shanghai Silaike Laboratory Animal Limited Liability Company. Kunming mice were obtained from New Drug Screening Center of China Pharmaceutical University. All the animals were pathogen free and allowed to access food and water freely. All the animal experiment was in accordance with Guide for the Care and Use of Laboratory Animals published by the National Institute of Health.

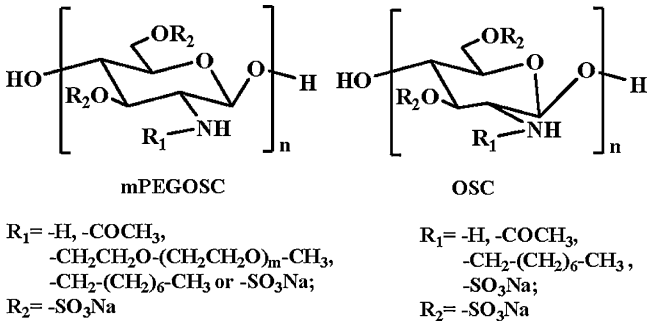

Fig. 1. The chemical structures of N-PEG-N-octyl-O-sulfate chitosan (mPEGOSC) and N-octyl-O-sulfate chitosan (OSC).

2.3. Synthesis and characterization of N-mPEG-N-octyl-O-sulfate chitosan (mPEGOSC)

A series of amphipathic chitosan derivates named N-mPEG-N-octyl-O-sulfate chitosan (mPEGOSC) were prepared and the general formula was shown in Fig. 1. The experimental details had been described in a previous paper (Yao et al., 2007). mPEG with different molecular weight of 1100, 2000 and 5000 were used and low, middle and high DS of mPEG groups were represented as L, M, H. Nine derivatives were synthesized with three molecular weights at three DS values of mPEG groups which were named mPEGOSC1100L, mPEGOSC1100M, mPEGOSC1100H, mPEGOSC2000L, mPEGOSC2000H, mPEGOSC5000L, mPEGOSC5000M and mPEGOSC5000H. The chemical structure and DS of the derivates were identified and calculated by ^{1}H NMR and ^{13}C NMR spectra (BRUKER AVANCE 500 AV system, Bruker Biospin GmbH, Rheinstetten, Germany), FT-IR spectra (Nicolet 2000 FT-IR spectrophotometer, Thermo Electron Corp., Madison, WI, USA). The molecular weights of mPEGOSCs were analyzed with gel-permeation chromatography (GPC) and Mn, Mw were obtained. Agilent 1100 series (Agilent Technologies, Palo Alto, CA, USA) with refractive index detector and a TOSOH TSK-G4000 PWxl column (7.8 mm × 30 cm) (TOSOH Corp., Tokyo, Japan) were used.

2.4. Preparation and characterization of PTX-loaded chitosan derivate micelles

PTX-loaded micelles based on mPEGOSC and OSC were prepared by dialysis method (Yao et al., 2007). Briefly, mPEGOSC or OSC was dissolved in water, PTX was dissolved in ethanol, and then the drug solution was injected into mPEGOSC or OSC solution with magnetic stirring at room temperature, the mixture was dialyzed against distilled water overnight at room temperature using dialysis membrane (MWCO 10,000). The micelle solution was filtered with a 0.22 μm pore-sized microfiltration membrane, then the PTX concentration had been analyzed by high-performance liquid chromatography (HPLC) and the lyophilized micelle powder was obtained. The HPLC was equipped with a reverse-phase column (4.6 mm × 250 mm, Hanbon, Jiangsu, China) at 40 °C and with a UV spectrophotometer (Agilent Technologies, Palo Alto, CA, USA). The mobile phase was a mixture of methanol and water (75:25 v/v). The samples were delivered at a flow rate of 1.0 ml/min and detected at a wavelength of 227 nm. A certain volume of PTX-loaded micelle solution was taken and redissolved with 50-fold volume mobile phase, and 20 μl of dilution was injected into the HPLC system. The PTX-loading rate in micelle was calculated by the following

equation:

$$\text{PTX-loading rate} = \frac{CV}{W_{\text{mPEGOSC}}} \times 100\%,$$

$$\text{Entrapment efficiency} = \frac{CV}{W_{\text{PTX}}} \times 100\%.$$

Where C, V, W_{mPEGOSC} and W_{PTX} represented the PTX concentration of micelle solution, the volume of micelle solution, the weight of micelles after freeze-drying and the weight of PTX feeded, respectively. Particle size and polydispersity index of the PTX-loaded micelles were measured using a Zetasizer 3000 HS instrument (Malvern Instruments, Malvern, UK) with 633 nm He-Ne lasers at 25 °C.

2.5. Pharmacokinetic studies of Taxol®, PTX-OSC and PTX-mPEGOSC in rats

Forty-five male Sprague–Dawley rats (180–230 g) were used to investigate the effect of formulations on the pharmacokinetics of PTX after intravenous administration. Rats were divided into 9 groups at random, and given a single 7 mg/kg body weight dose of every formulation, including Taxol®, PTX-OSC, PTX-mPEGOSC1100L, PTX-mPEGOSC1100M, PTX-mPEGOSC1100H, PTX-mPEGOSC2000L, PTX-mPEGOSC2000M, PTX-mPEGOSC2000H, PTX-mPEGOSC5000L, by tail-vein injection (mPEGOSC5000M and mPEGOSC5000H could not constructed micelles to solubilize the PTX). Each formulation was tested on 5 rats. The concentrations of PTX in PTX-mPEGOSCs and PTX-OSC solutions for pharmacokinetic study were 2 mg/ml. As the control, Taxol® was diluted to 2 mg/ml with 5% glucose solution before administration. 0.4 ml of blood samples were collected into heparinized tubes from the fossa orbitalis at 0 min (predose), 0.083, 0.25, 0.5, 0.75, 1, 2, 4, 6, and 8 h after intravenous administration. 200 μl of blood sample, 100 μl of internal standard (Norethisterone in methanol) and 700 μl of 50% acetonitrile in water were added into a protein precipitation tube. The mixture was vortexed for 4 min and centrifugated at 8000 rpm for 5 min. 500 μl of the supernatant was injected into glass centrifuge tube, 3 ml acetoacetate was added and followed by vortex for 2 min. The mixture was centrifugated at 3000 rpm for 10 min and the supernatant was collected and blowed to dry using nitrogen. And then, 100 μl mobile phase was added, the solution was centrifugated at 15,000 rpm for 5 min after vortex. 50 μl of the solution was injected onto the HPLC system. The concentrations of PTX in samples were analyzed under the condition described in Section 2.4. The intraday and interday precision, specificity and accuracy of the HPLC method were validated before sample analysis. The PTX plasma concentrations over times were analyzed by compartmental analysis using the standard software package program 3P97 (the Committee of Mathematic Pharmacology of the Chinese Society of Pharmacology) and the following parameters of pharmacokinetics were obtained: area under the plasma concentration time curve (AUC), plasma half life (T1/2), total plasma clearance (Cls), apparent distribution volume (Vd), and rate constant of elimination phase (β), etc. Mean residence time (MRT) was calculated by non-compartmental method of statistical quadrature method.

2.6. Tissue distribution studies

One hundred sixty-two female Kunming mice (18–22 g) were used in the tissue distribution studies of PTX in three formulations (Taxol®, PTX-OSC and PTX-mPEGOSC2000M) after intravenous administration via caudal vein at the dose of 10 mg/kg body weight. All mice were divided into 27 groups at random. 9 groups combined randomly were treated with one formulation, and at every sample point, 6 mice in one group were sacrificed by cervical dislocation after drowing blood from the eyeball. Following closely, the blood was immediately treated as described in Section 2.5. The organs of heart, liver, spleen, lung, kidney and uterus (including ovary) were excised and thoroughly washed with double distilled water, then blotted dry and weighed. Subsequently, the weighted tissues were homogenized (Tearork, BioSpec Products Inc., Bartlesville, OK) with 2-fold weight of normal saline. 100 μl of homogenate, 100 μl of internal standard (Norethisterone in acetonitrile) and 100 μl of acetonitrile were added into a glass tube. The mixture was vortexed for 4 min and centrifugated at 15,000 rpm for 5 min. 50 μl of the supernatant was injected onto the HPLC system. The concentrations of PTX in samples were analyzed under the condition described in Section 2.4. The drug concentration in blood and tissues were assayed using HPLC with the injected volume of 50 μl. The pharmacokinetic parameters of blood, heart, liver, spleen, lung, kidney and uterus (including ovary) were calculated using statistical moment method.

2.7. Dissociation kinetic of PTX-loaded micelles below CMC

Micelle dissociation below the CMC was performed as a fluorescent probe. The pyrene-loaded micelle solution was prepared as following. Pyrene was dissolved in acetone at 3×10^{-5} M as stock solution, and eight derivates, OSC, mPEGOSC1100L, mPEGOSC1100M, mPEGOSC1100H, mPEGOSC2000L, mPEGOSC2000M, mPEGOSC2000H and mPEGOSC5000L were dissolved in PBS (0.5 M, pH 7.4) at the concentration of 100 times of respective CMC, respectively. 100 μl of pyrene solution was dropwised into polymer micellar solution following by stirring at room temperature for 3 h at 65 °C. The final concentration of pyrene was 6×10^{-7} M in all test samples which was lower than the saturated solubility of it in PBS (0.5 M, pH 7.4). 20 μl pyrene-loaded micelle solutions was injected into 3.0 ml PBS (0.5 M, pH 7.4) upon stirring at 37 °C, the change in pyrene fluorescence intensity at the defined λ_{em} and λ_{ex} was recorded from the initial time (I_0) to 600 s with interval of 5 s using a Shimadzu RF-5301 PC spectrofluorometer at 37 °C. At time t, the fluorescent intensity was I_t. Then the samples were sealed and stored in dark. The fluorescence intensities of pyrene in the samples were recorded at 7, 8 and 9 days to identify the infinite fluorescence intensity (I_i). The excitation spectrum might undergo a determinate shift to longer wavelengths if the probe escaped from a hydrophobic to a hydrophilic environment. So the excitation spectrum of the solution was scanned again from 300 to 360 nm at λ_{em} of 390 nm at 7, 8 and 9 days to track the end of dissociation of pyrene-loaded micelle. At time t, the fraction of intact micelles (f_t) was calculated from the following equation: $f_t = (I_t - I_i)/(I_0 - I_i)$. Both micelle dissociation and pyrene diffusion from the intact micelles might decrease fluorescence intensity of pyrene. To eliminate the influence of diffusion of pyrene from the intact micelles, an independent experiment was designed in parallel as follows, 20 μl pyrene-loaded micelle solutions was injected into 3.0 ml of the corresponding blank micelle solutions at the same polymer concentration. As the micelles will not dissociate when mixed with the same micelles at the same concentration, the measured change of fluorescence intensity over time was attributed to diffusion of pyrene from intact micelles, which was compensated when calculated the I_t values of samples.

2.8. Statistical analysis

Statistical comparisons were performed by Student's t-test for two groups, and one-way ANOVA for multiple groups. Values of

Table 1
The molecular weights, DS values (mol/kg), CMC values of mPEGOSCs, OSC and the dissociation dynamics parameters of micelles.

Compound	Molecular weight		DS (mol/kg)				Dynamics parameters		CMC (mg/ml)
	Mn	Mw	mPEG	Octyl	Sulfate	Chitosan	k (1/s)	$f_{t,\ 10\ min}$	
OSC	3.57×10^6	6.24×10^6	0.45	0	0.45	2.00	0.0035	0.77	0.45
mPEGOSC1100L	6.06×10^6	9.29×10^6	0.015	6.46	0.015	1.53	0.0086	0.675	0.015
mPEGOSC1100M	3.01×10^6	5.51×10^6	0.015	9.06	0.015	1.25	0.0117	0.563	0.015
mPEGOSC1100H	3.37×10^6	5.79×10^6	0.022	10.84	0.022	1.07	0.0164	0.468	0.022
mPEGOSC2000L	1.63×10^5	1.86×10^6	0.015	4.15	0.015	1.75	0.0057	0.682	0.015
mPEGOSC2000M	2.46×10^5	1.73×10^6	0.011	6.4	0.011	1.43	0.008	0.667	0.011
mPEGOSC2000H	7.49×10^5	3.15×10^6	0.019	8.74	0.019	1.26	0.0135	0.518	0.019
mPEGOSC5000L	3.70×10^6	5.69×10^6	0.030	11.75	0.030	1.06	0.0235	0.334	0.030
mPEGOSC5000M	2.39×10^6	4.08×10^6	0.42	15.68	1.56	0.61	/	/	/
mPEGOSC5000H	3.96×10^6	6.35×10^6	0.2	17.64	1.18	0.48	/	/	/

Table 2
PTX-loading rate, entrapment efficiency, particle size and polydispersity index of PTX-loaded micelles (mean ± S.D., $n = 3$).

Compound	PTX-loading rate (%, w/w)	Entrapment efficiency (%, w/w)	Particle size (nm)	Polydispersity index
mPEGOSC1100L	37.6 ± 1.0	72.3 ± 2.5	119.0 ± 1.9	0.28 ± 0.02
mPEGOSC1100M	38.9 ± 0.8	77.2 ± 2.4	117.7 ± 1.1	0.30 ± 0.01
mPEGOSC1100H	37.9 ± 1.5	74.8 ± 4.4	119.6 ± 2.2	0.28 ± 0.05
mPEGOSC2000L	41.8 ± 0.2	84.4 ± 2.9	108.5 ± 0.6	0.34 ± 0.04
mPEGOSC2000M	41.1 ± 2.0	82.3 ± 4.9	104.3 ± 5.8	0.39 ± 0.12
mPEGOSC2000H	42.6 ± 0.9	85.6 ± 3.0	110.6 ± 1.2	0.34 ± 0.05
mPEGOSC5000L	38.5 ± 0.5	76.4 ± 1.8	133.4 ± 0.6	0.34 ± 0.03

$p < 0.05$ and $p < 0.001$ were considered statistically significant and highly significant, respectively.

3. Results and discussions

3.1. Synthesis and characterization of N-mPEG-N-octyl-O-sulfate chitosan (mPEGOSC)

The chemical structure of mPEGOSC was briefly shown in Fig. 1 and identified by ^{1}H NMR spectra, ^{13}C NMR spectra and FT-IR spectra. A DS value of different group (mol/mol) was calculated from molar ratio of C/N and S/N obtained from elemental analysis. The DS values of mPEG, octyl and sulfate group (mol/kg) were calculated from the DS value of different group (mol/mol) and shown in Table 1, and the molecular weights, CMC values of mPEGOSCs and OSC were also listed in Table 1.

3.2. Preparation and characterization of PTX-loaded chitosan micelles

Dialysis method was used to prepare drug-loaded micelle solutions based on chitosan derivates, and the drug-loaded micelle powder was obtained via lyophilization. PTX-loading rate, entrapment efficiency, particle size and polydispersity index of drug-loaded micelles were listed in Table 2. Micelles based on mPEGOSC2000s had the highest PTX-loading rates (41.1–42.6%), entrapment efficiencies (82.3–85.6%) and the smallest particle sizes (104.3–110.6 nm). X-ray powder diffraction was used to further characterize drug-loaded micelles. As shown in Fig. 2, diffraction peaks characteristics of PTX, which were visible between 5° and 25° in the patterns obtained for the physical mixture of PTX and chitosan derivatives, disappeared in the pattern of PTX-loaded micelles. Although typical crystal peaks for PTX in physical mixture were weakened, the mixture did not achieve dispersion at molecular level. All this indicated that PTX was encapsulated in the polymeric micelles in molecular or amorphous state and there was no free drug in the surface of micelles.

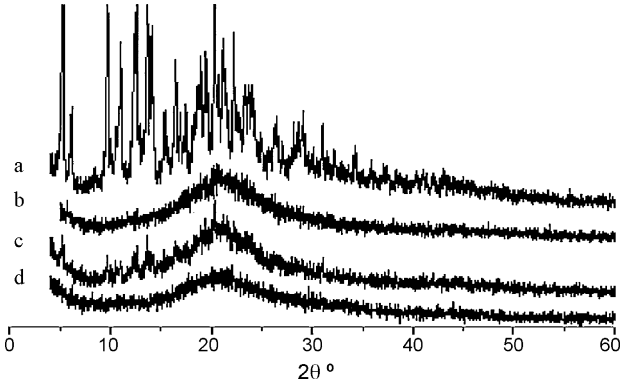

Fig. 2. WAXD spectra of (a) paclitaxel, (b) mPEGOSC2000M, (c) physical mixture of paclitaxel and mPEGOSC2000M (2:3 (w/w)) and (d) PTX-mPEGOSC2000M micelles (PTX-loading rate = 41.6%).

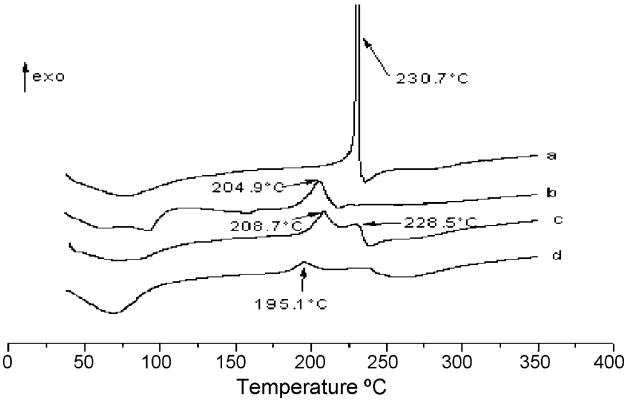

Fig. 3. DSC spectra of (a) mPEGOSC2000M, (b) paclitaxel, (c) physical mixture of paclitaxel and mPEGOSC2000M (2:3 (w/w)) and (d) PTX-mPEGOSC2000M micelles (PTX-loading rate = 41.6%).

DSC thermograms (Fig. 3) revealed PTX exothermic peak at 204.9 °C and mPEGOSC2000M exothermic peak at 230.7 °C. For physical mixture, both peaks were observed with small shifts at 208.7 and 228.5 °C, respectively. The lyophilized drug-loaded micelles showed no characteristic exothermic peak for PTX and mPEGOSC2000M, instead, a new peak at 230 °C appeared, which suggested that a new solid dispersion of PTX and the polymer was formed during the freeze-drying.

Size and size distribution of PTX-loaded micelles based on mPEGOSCs and OSC were measured by DLS, which were shown in Table 2.

3.3. In vivo–in vitro correlations of PTX-loaded micelles

3.3.1. Structural integrity of drug-loaded micelles in rat plasma

Stability of the drug-loaded micelles in rat plasma was tested to supply substantial information for the reasonable evaluation to the pharmacokinetics and tissue distributions of the encapsulated drug. It was believed that the intact structure of micelles would be a prerequisite for the passive targeting effect.

Excitation spectrum of the solution was scanned from 300 to 360 nm fixing the emission wavelength (λ_{em}) at 390 nm, from which the excitation wavelength (λ_{ex}) was set at 339 nm. Fluorescence intensity of pyrene (λ_{ex} = 339 nm, λ_{em} = 390 nm) was recorded every 5 s from the initial time to 600 s. And fluorescence intensity of pyrene in every group kept stable through the test until 10 min, the RSD values of all groups were less than 0.3%. Pyrene encapsulated within the cores of micelles might escape into the medium after the micelle dissociation, which resulted in decreased fluorescence intensity, therefore the stable fluorescence intensity within 10 min indicated that no pyrene released or leaked from the micelle, and micelles incubated in rat plasma at established dilutability maintained intact structure.

This result sustained that the dissociation of drug-loaded micelles within 10 min was induced by dilution.

3.3.2. Dissociation kinetic of PTX-loaded micelles below CMC

Dissociation kinetics of preformed micelles was one of the basic factors which might determine the circulation time in blood and remodel the biodistribution of encapsulated drug. It was essential to reveal the relationship between the chemical composition of the chitosan derivates and the stability of micelles below CMC, furthermore, the pharmacokinetic parameters were investigated as a function of the dissociation kinetics parameters. The dissociation of PTX-loaded micelles below CMC was monitored by the change in the fluorescent intensity of pyrene (λ_{ex} = 339 nm, λ_{em} = 390 nm). The f_t–time curves of eight micellar systems were shown in Fig. 4.

The micelle dissociation proceeded very rapidly for the first 5 min, and then slowed down. The rate of dissociation followed first-order kinetics in the initial 30 s for all these micelles, and the dissociation constants (k) were shown in Table 1. After 50 s, fluorescence intensity of pyrene decreased more slowly and at 10 min the fraction of intact micelles mimicked a constant value ($f_{t,\,10\,min}$), which was set as a characteristic parameter for the evaluation of micelle dissociation below CMC. Fig. 5 shown that the two dissociation kinetic parameters k and $f_{t,\,10\,min}$ were highly linearly correlated with the DS of chitosan unit (mol/kg), which was inducted to estimate the grafting degree of a series of mPEGOSCs.

The micelles based on mPEGOSC with higher DS of chitosan unit (mol/kg) shown slower dissociation when diluted below CMC, and higher stability in blood was presumed for this reason. For the micelles constructed by small molecular surfactants, the rate constant of dissociation were on the order of 10^2 s^{-1}, which was much larger than the polymeric micelles, especially, than the graft copolymer micelles (Wang et al., 1992). Intensive dissociation in the initial

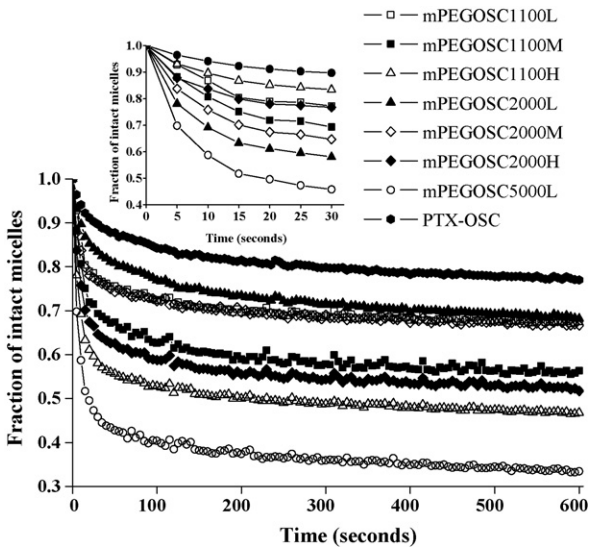

Fig. 4. Fraction of micelles (f_t) that remained upon dilution below CMC as a function of time.

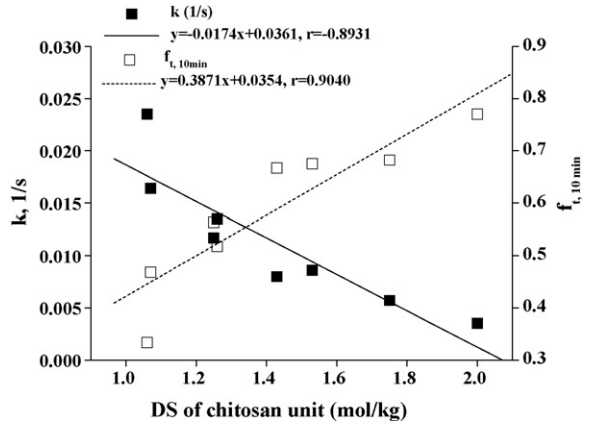

Fig. 5. The linear regression curves of k versus DS of chitosan unit (mol/kg) and $f_{t,\,10\,min}$ versus DS of chitosan unit (mol/kg), respectively.

stage was observed in most block copolymer micelles when diluted below CMC (Tao and Uhrich, 2006). The observed slow dissociation for mPEGOSC or OSC micelles was likely due to the stable backbone of chitosan, which drastically coupled in the corona and core of these micelles. Therefore, the mPEGOSC or OSC micelles had better tolerance to high dilution.

3.4. Pharmacokinetic studies of Taxol®, PTX-OSC and PTX-mPEGOSC in rats

The pharmacokinetic parameters for PTX in plasma were estimated by compartmental method shown in Table 3. The mean values of PTX concentrations in plasma samples at different collection times were used to determine the appropriate compartmental model. The goodness of fit for each model was distinguished by the value of AIC, the optimum compartment model was determined with minimum AIC value. If there was no significant difference between the optimum compartment model and suboptimum compartment model, the simple compartment model was selected. Two-compartment model was the optimum for the nine formulations with the weight of 1/C which regarded both the higher and lower concentrations. The Vd value of PTX-mPEGOSC2000L was 404.6 ± 65.3 ml/kg, which was the smallest in the PTX-mPEGOSCs

Table 3
The main pharmacokinetics parameters of PTX in blood for Taxol®, PTX-OSC, and PTX-mPEGOSCs (mean ± S.D., $n = 5$).

Parameters	PTX-OSC	Taxol®	PTX-mPEGOSC1100L	PTX-mPEGOSC1100M	PTX-mPEGOSC1100H
α[a] (1/h)	6.028 ± 0.340	4.380 ± 0.786**	4.536 ± 0.31**	13.50 ± 1.84**	4.577 ± 0.217**
β[b] (1/h)	0.2776 ± 0.012	0.4157 ± 0.0622**	0.2754 ± 0.0238	0.2970 ± 0.0319	0.3468 ± 0.0223**
Vd[c] (ml/kg)	692.9 ± 94.9	349.2 ± 27.8**	484.6 ± 62.4**	491.1 ± 61.5**	496.8 ± 73.5**
T1/2α[d] (h)	0.1153 ± 0.0063	0.1627 ± 0.0313*	0.1534 ± 0.0113**	0.1525 ± 0.0166**	0.1517 ± 0.0074**
T1/2β[e] (h)	2.501 ± 0.109	1.695 ± 0.231**	2.533 ± 0.238	2.357 ± 0.268	2.006 ± 0.133**
CL[f] (ml/h/kg)	1908.3 ± 268.8	583.6 ± 75.9**	1079.8 ± 159.2**	1160.1 ± 201.9**	1272.0 ± 203.1**
AUC (0–∞)[g] (μg h/ml)	3.83 ± 0.52	12.84 ± 1.68**	6.83 ± 1.0**	6.40 ± 1.18**	5.87 ± 0.93**
AUC (0–t_n)[h] (μg h/ml)	3.49 ± 0.45	12.34 ± 1.70**	6.39 ± 0.88**	6.04 ± 1.10**	5.62 ± 0.87**
MRT (0–∞)[i] (h)	2.441 ± 0.086	1.818 ± 0.268**	2.053 ± 0.150**	1.906 ± 0.044**	1.590 ± 0.074**
MRT (0–t_n)[j] (h)	1.460 ± 0.027	1.433 ± 0.102	1.391 ± 0.023**	1.311 ± 0.017**	1.143 ± 0.037**
MRT (0–t_n)[j] (h)	1.460 ± 0.027	1.433 ± 0.102	1.391 ± 0.023**	1.311 ± 0.017**	1.143 ± 0.037**

Parameters	PTX-mPEGOSC2000L	PTX-mPEGOSC2000M	PTX-mPEGOSC2000H	PTX-mPEGOSC5000L
α[a] (1/h)	4.142 ± 0.237**	4.055 ± 0.185**	3.977 ± 0.302**	3.906 ± 0.274**
β[b] (1/h)	0.2754 ± 0.0146**	0.2555 ± 0.0116**	0.3055 ± 0.0099**	0.4688 ± 0.0461**
Vd[c] (ml/kg)	404.6 ± 65.3**	412.0 ± 93.7**	421.2 ± 107.4**	417.0 ± 87.6**
T1/2α[d] (h)	0.1678 ± 0.0099**	0.1712 ± 0.0079**	0.1751 ± 0.0130**	0.1782 ± 0.0128**
T1/2β[e] (h)	2.523 ± 0.139	2.718 ± 0.125*	2.271 ± 0.074**	1.490 ± 0.144**
CL[f] (ml/h/kg)	719.7 ± 153.9**	670.2 ± 152.8**	807.4 ± 207.5**	989.3 ± 219.0**
AUC (0–∞)[g] (μg h/ml)	10.41 ± 2.21**	11.31 ± 2.49**	9.53 ± 2.38**	7.72 ± 1.77**
AUC (0–t_n)[h] (μg h/ml)	9.73 ± 2.11**	10.21 ± 2.12**	8.99 ± 2.20**	7.63 ± 1.73**
MRT (0–∞)[i] (h)	2.235 ± 0.058**	2.670 ± 0.240	1.949 ± 0.131**	1.063 ± 0.029**
MRT (0–t_n)[j] (h)	1.573 ± 0.017**	1.669 ± 0.049**	1.392 ± 0.066	0.950 ± 0.016**

[a] Rate constant of distribution phase.
[b] Rate constant of elimination phase.
[c] Apparent volume of distribution.
[d] Apparent plasma half-life (Tt1/2) of distribution phase (α-phase).
[e] Apparent plasma half-life (T1/2) of elimination phase (β-phase).
[f] Total body clearance.
[g] The area under the plasma concentration–time curve from time 0 to the last time point examined.
[h] The area under the plasma concentration–time curve from time 0 to time infinity.
[i] Mean residence time from time 0 to the last time point examined.
[j] Mean residence time from time 0 to time infinity.
* $p < 0.05$ versus PTX-OSC.
** $p < 0.01$ versus PTX-OSC.

but higher than Taxol®, followed by PTX-mPEGOSC2000M of 412.0 ± 93.7 ml/kg, and that of OSC was 692.9 ± 94.9 ml/kg. Comparing with PTX-OSC and PTX-mPEGOSC, Taxol® provided Vd value of 349.2 ± 27.8. The Cls of PTX-mPEGOSC2000M was estimated at 670.2 ± 152.8 ml/h/kg which was 1.15-fold higher than Taxol® and a 2.85-fold lower than PTX-OSC. The AUC (0–t_n) of PTX-mPEGOSC2000M was 10.21 ± 2.12 μg h/ml, which were 2.93 times higher than PTX-OSC and 0.83 times lower than Taxol®. PTX-mPEGOSC2000M provided the longest MRT in all the groups, which was 1.16 times longer than Taxol®. For the micelles based on mPEGOSCs or OSC, the dissociation dynamics of micelles below CMC dominated the rate constant of elimination phase (β). Fig. 6 illustrated the inverse linear relationship obtained between the logarithmic β value and $f_{t,\,10\,min}$, which indicated that the micelles based on chitosan derivates with high DS of chitosan unit (mol/kg) might retard the decrease of PTX concentration in elimination phase. The AUC of PTX was mainly dependent on rate constant of distribution phase (α), but also subjected to secondary influence from β value. Mainly, slower elimination in the initial stage of intravenous injection was induced by the greater stabilization effect which provided by mPEG group, and the micelles based on mPEGOSC2000 and mPEGOSC5000 had greater AUC. Secondly, the micelle formed from the chitosan derivates with high DS of chitosan unit (mol/kg) slowed down the elimination of PTX in the later stage of intravenous injection, which contributed to a greater AUC.

The characteristics for rapid elimination in the initial phase of intravenous injection was evaluated by α value, a higher α value indicated more rapid elimination of PTX from the blood circulation. In the classical sense, phagocytosis is receptor-mediated, actin-driven proceeds (Aderem and Underhill, 1999). Adsorption of plasma protein on the surface of micelles might mediate enhanced phagocytosis by RES. By means of PEGylation, drug-loaded micelles were protected from recognition and phagocytosis by RES, which increased α value. PEGylation would decrease the DS of chitosan unit (mol/kg) of chitosan derivatives, and higher DS of chitosan unit (mol/kg) was considered to be beneficial to the rigidity of micelles, consequently, lower degree of PEGylation would be advantageous

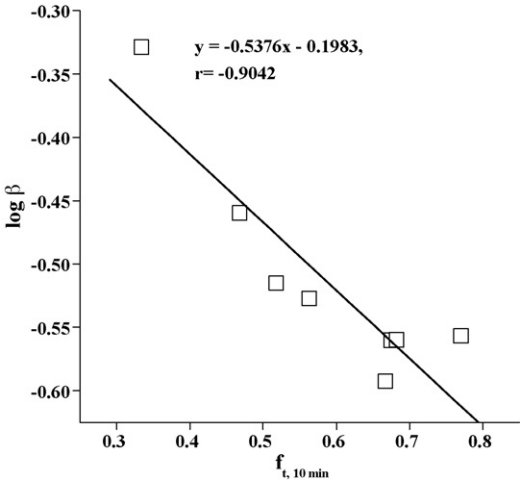

Fig. 6. The linear regression curves of log β versus $f_{t,\,10\,min}$.

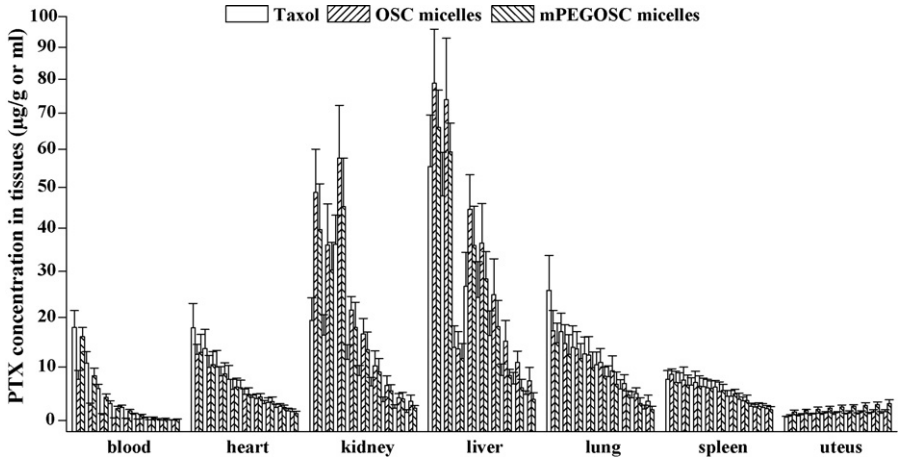

Fig. 7. The PTX concentration of three groups (Taxol®, PTX-OSC and PTX-mPEGOSC2000M) in tissues at different time points (0.083, 0.25, 0.5, 0.75, 1, 2, 4, 6 and 8 h) (mean ± S.D., $n = 6$).

Table 4
AUC ($0–t_n$) and MRT ($0–t_n$) of Taxol®, PTX-OSC and PTX-mPEGOSC2000M in blood and tissues ($n = 6$).

Tissues	AUC ($0–t_n$)[a] (μg h/ml or μg h/g)			MRT ($0–t_n$)[b] (h)		
	Taxol®	PTX-OSC	PTX-mPEGOSC2000M	Taxol®	PTX-OSC	PTX-mPEGOSC2000M
Blood	12.474	3.219	10.481	1.208	1.074	1.424
Heart	32.978	29.880	30.417	2.622	2.909	2.791
Liver	109.795	174.058	121.547	2.395	2.466	2.130
Spleen	31.613	30.305	30.589	3.172	3.090	3.114
Lung	55.220	60.310	43.103	2.711	3.020	2.769
Kidney	40.623	78.739	66.250	2.346	2.296	2.295
Uterus	9.346	11.926	21.239	/	/	/

[a] The area under the plasma concentration–time curve from time 0 to the last time point examined.
[b] Mean residence time from time 0 to the last time point examined.

to greater rigidity of micelles. Greater rigidity would slowed down the dissociation of micelle after injected into blood circulation, and the dissociation of micelles was considered to contribute to the release and consequently to the elimination of the drug. In summary, the inverse correlation between DS of chitosan unit (mol/kg) and β value was accessible. The comprehensive effect was that the AUC ($0–t_n$) values of PTX-mPEGOSC were much greater than that of PTX-OSC ($p < 0.01$).

3.5. Tissue distribution studies

PTX concentrations investigated in blood and organs of heart, liver, spleen, lung, kidney and uterus (including ovary), after i.v. administration of 10 mg equivalent PTX/kg body weight for PTX-loaded micelles and Taxol®, which were presented in Fig. 7. The observed PTX concentrations in blood and tissues were estimated to obtain the pharmacokinetic parameters by statistical moment analysis. The maximum concentration (C_{max}) (μg/ml or μg/g) and the time of maximum concentration (T_{max}) (h) values were obtained from visual inspection of the data. Table 4 summarized the AUC ($0–t_n$) and MRT ($0–t_n$) values of PTX in various tissues and blood.

The PTX concentrations in blood changed over time were shown in Fig. 7, which demonstrated the same trends revealed in pharmacokinetic studies. The PTX concentrations of PTX-mPEGOSC2000M group were higher than Taxol® group after 4 h. Higher PTX concentrations of PTX-OSC group in liver were maintained through 8 h, and the PTX concentrations of PTX-mPEGOSC2000M group decreased lower than Taxol® group after 6 h. The PTX concentrations of PTX-mPEGOSC2000M group in lung maintained a lower level than the other two groups through 8 h. Table 4 also demonstrated lower AUC ($0–t_n$) values for PTX-mPEGOSC2000M and Taxol® groups in liver and lung than PTX-OSC group. Therefore, the micelles based on pegylated chitosan derivates greatly decreased the elimination by the RES and accumulation in the liver and spleen. The AUC ($0–t_n$) values of PTX-OSC and PTX-mPEGOSC2000M in heart were 0.906 and 0.922-fold lower than that of Taxol®, but 1.938 and 1.631 times higher in kidney. Compared with Taxol®, PTX-mPEGOSC2000M might decrease the toxic effect in heart, and the toxic effect of PTX-mPEGOSC2000M to kidney might also improve compared with PTX-OSC. At all sample points, the PTX concentrations of PTX-mPEGOSC2000M group were higher than the other two groups in uterus, and the AUC ($0–t_n$) of PTX-mPEGOSC2000M was 2.272 times higher than that of Taxol®. It was calculated that the targeting efficiency of PTX-mPEGOSC2000M to uterus was higher than Taxol®, which indicated that PTX-mPEGOSC2000M provided lower PTX level in blood and other tissues compared with Taxol® when achieved same amount of PTX in uterus.

4. Conclusion

In this study, a series of novel chitosan derivates with hydrophobic moiety of octyl and hydrophilic moieties of sulfate and mPEG were synthesized to assemble micelles, which was compared with PTX-loaded micelles based on OSC. The introduction of mPEG block decreased plasma protein adhesion and phagocytosis by RES and increase the circulation time of micelles after intravenous administration. AUC ($0–t_n$) of PTX-mPEGOSC2000M was 2.93 times higher than PTX-OSC and 0.83 times lower than Taxol®. Introduction of PEG groups decreased the adsorption of plasma protein to micelle, PEG of molecular weight 2000 and 5000 brought the similar effect but stronger than molecular weight 1100. Similar effect was observed between the different DS with the same PEG molec-

ular weight. Slower elimination in the initial stage of intravenous injection was induced by the greater stabilization effect which provided by mPEG2000 or mPEG5000 groups, and the micelle formed from the chitosan derivates with high DS of chitosan unit (mol/kg) slowed down the elimination of PTX in the later stage of intravenous injection. Of note, higher targeting efficiency of PTX-mPEGOSC2000M to uterus (including ovary) was estimated in the tissue distribution studies in mice compared with Taxol®. Therefore, the PTX-mPEGOSC was expected to be a potential drug delivery system of PTX for chemotherapy of ovarian cancer.

Acknowledgements

This study is financially supported by National Natural Science Foundation of China (30772662), Program for New Century Excellent Talents in University (NCET-06-0499), Ministry of Education key project (107062), grant from the Ph.D. Programs Foundation (20070316004) and 111 Project from the Ministry of Education of China and the State Administration of Foreign Expert Affairs of China (No. 111-2-07).

References

Aderem, A., Underhill, D.M., 1999. Mechanisms of phagocytosis in macrophages. Annu. Rev. Immunol. 17, 593–623.

Ceruti, M., Crosasso, P., Brusa, P., Arpicco, S., Dosio, F., Cattel, L., 2000. Preparation, characterization, cytotoxicity and pharmacokinetics of liposomes containing water-soluble prodrugs of paclitaxel. J. Control. Release 63, 141–153.

Croy, S.R., Kwon, G.S., 2006. Polymeric micelles for drug delivery. Curr. Pharm. Des. 12, 4669–4684.

Hamaguchi, T., Matsumura, Y., Suzuki, M., Shimizu, K., Goda, R., Nakamura, I., Nakatomi, I., Yokoyama, M., Kataoka, K., Kakizoe, T., 2005. NK105, a paclitaxel incorporating micellar nanoparticle formulation, can extend in vivo antitumour activity and reduce the neurotoxicity of paclitaxel. Br. J. Cancer 92, 1240–1246.

Hawkins, M.J., Shiong, P.S., Desai, N., 2008. Protein nanoparticles as drug carriers in clinical medicine. Adv. Drug Deliv. Rev. 60, 876–885.

Hennenfent, K.L., Govindan, R., 2005. Novel formulations of taxanes: a review. Old wine in a new bottle? Ann. Oncol. 17, 735–749.

Kan, P., Chen, Z.B., Lee, C.J., Chu, I.M., 1999. Development of nonionic surfactant/phospholipid o/w emulsion as a paclitaxel delivery system. J. Control. Release 58, 271–278.

Kim, S.C., Kim, D.W., Shim, Y.H., Bang, J.S., Oh, H.S., Kim, S.W., Seo, M.H., 2001. In vivo evaluation of polymeric micellar paclitaxel formulation: toxicity and efficacy. J. Control. Release 72, 191–202.

Mahmud, A., Xiong, X.B., Aliabadi, H.M., Lavasanifar, A., 2007. Polymeric micelles for drug targeting. J. Drug Target. 15, 533–584.

Marupudi, N.I., Han, J.E., Li, K.W., Renard, V.M., Tyler, B.M., Brem, H., 2007. Paclitaxel: a review of adverse toxicities and novel delivery strategies. Expert Opin. Drug Saf. 6, 609–621.

Otsuka, H., Nagasaki, Y., Kataoka, K., 2003. PEGylated nanoparticles for biological and pharmaceutical applications. Adv. Drug Deliv. Rev. 55, 403–419.

Panchagnula, R., 1998. Pharmaceutical aspects of paclitaxel. Int. J. Pharm. 172, 1–15.

Singla, A.K., Garg, A., Aggarwal, D., 2002. Paclitaxel and its formulations. Int. J. Pharm. 235, 179–192.

Tao, L., Uhrich, K.E., 2006. Novel amphiphilic macromolecules and their in vitro characterization as stabilized micellar drug delivery systems. J. Colloid Interf. Sci. 298, 102–110.

Vlerken, E., Vyas, K., Amiji, M., 2007. Poly(ethylene glycol)-modified nanocarriers for tumor-targeted and intracellular delivery. Pharm. Res. 24, 1405–1414.

Wang, J., Mongayt, D., Torchilin, V.P., 2005. Polymeric micelles for delivery of poorly soluble drugs: preparation and anticancer activity in vitro of paclitaxel incorporated into mixed micelles based on poly(ethylene glycol)-lipid conjugate and positively charged lipids. J. Drug Target. 13, 73–80.

Wang, Y., Balaji, R., Quirk, R.P., Mattice, W.L., 1992. Detection of the rate of exchange of chains between micelles formed by diblock copolymers in aqueous solution. Polym. Bull. 28, 333–338.

Wrasidlo, W., Gaedicke, G., Guy, R.K., Renaud, J., Emmanuel, P., Nicolaou, K.C., Reisfeld, R.A., Lode, H.N., 2002. A novel 2′-(N-methylpyridinium acetate) prodrug of paclitaxel induces superior antitumor responses in preclinical cancer models. Bioconjug. Chem. 13, 1093–1099.

Yao, Z., Zhang, C., Ping, Q., Yu, L., 2007. A series of novel chitosan derivatives: synthesis, characterization and micellar solubilization of paclitaxel. Carbohyd. Polym. 68, 781–792.

Zhang, C., Ping, Q.N., Zhang, H.G., Shen, J., 2003. Preparation of *N*-alkyl-*O*-sulfate chitosan derivatives and micellar solubilization of taxol. Carbohyd. Polym. 54, 137–141.

Zhang, C., Qineng, P., Zhang, H., 2004. Self-assembly and characterization of paclitaxel-loaded *N*-octyl-*O*-sulfate chitosan micellar system. Colloids Surf. B: Biointerfaces 25, 69–75.

Zhang, C., Qu, G., Sun, Y., Wu, X., Yao, Z., Guo, Q., Ding, Q., Yuan, S., Shen, Z., 2008a. N-octyl-O-sulfate chitosan micelles loaded with paclitaxel. Biomaterials 29, 1233–1241.

Zhang, C., Qu, G., Sun, Y., Yang, T., Yao, Z., Shen, W., Shen, Z., Ding, Q., Zhou, H., Ping, Q., 2008b. Biological evaluation of N-octyl-O-sulfate chitosan as a new nano-carrier of intravenous drugs. Eur. J. Pharm. Sci. 33, 415–423.

Zhang, X., Burt, H.M., Mangold, G., Von Hoff, D., Mayer, L., Hunter, W.L., 1997. Anti-tumor efficacy and biodistribution of intravenous polymeric micellar paclitaxel. Anti-cancer Drug 8, 696–701.

Zhang, X., Jackson, J.K., Burt, H.M., 1996. Development of amphiphilic diblock copolymers as micellar carriers of taxol. Int. J. Pharm. 132, 195–206.